Journal of Information Display
Vol. 12, No. 4, December 2011, 179–190

Color display evaluation *vs.* viewing angle using $L^*a^*b^*$ color space and Fourier-optics measurements

Pierre Boher[a*] Thierry Leroux[a], Thibault Bignon[a] and Pierre Blanc[b]

[a]*ELDIM, 1185 Rue d'Epron, F14200 Hérouville Saint Clair, France;* [b]*Laboratoires d'Essais de la FNAC, 12 rue Jean Antoine de Baïf, 75013 Paris, France*

(*Received 4 July 2011; Revised 22 August 2011; Accepted 26 August 2011*)

A complete analysis of the color-viewing-angle properties of different displays is presented herein using color-viewing-angle measurements made with a Fourier-optics system. The color gamut in the CIE $u'v'$ chromatic plane was computed for all the viewing angles. The introduction of the lightness using the $L^*a^*b^*$ color space allowed a more precise analysis of the emissive properties of each display. The displays can be directly compared using a common reference. The viewing-angle dependence can be analyzed in full detail using the on-axis values as reference. The gravity center behavior and area of the color hull were computed for a more precise evaluation and comparison.

Keywords: color; gamut; lab; viewing angle

1. Introduction

The optical characterization of displays is gaining greater importance for quality control and comparison of different technologies. A greater variety of display devices is available from an increasing number of display makers, and new technologies for image quality improvement and cost reduction are continuously being developed. The viewing angle and color quality are certainly among the most important specifications. Since their introduction to the market by ELDIM more than 15 years ago, Fourier-optics-based viewing-angle instruments have been recognized as powerful tools for measuring the aforementioned important characteristics [1,2]. The last-generation instruments are now able to measure the light emitted by the display up to $\pm 88°$ for all the azimuths on large spot sizes of up to 6 mm. For autostereoscopic 3D displays, a dedicated Fourier-optics instrument with an ultrahigh angular resolution has also been developed [3]. Each of these systems can measure the luminance and color, and even the radiance in some cases [4,5]. The color measurements are made using a monochrome CCD and color filters spectrally matched to the Commission International de L'Eclairage (CIE) curves to ensure maximum accuracy in each system. Additional color calibrations allow very-high-accuracy color measurements for the entire angular aperture [6].

The simplest evaluation of the viewing angle has been made using luminance measurement *vs.* angle since the onset of the LCD displays. Nevertheless, the luminance contrast criteria are no longer sufficient to express the quality of the current displays. The color quality has been checked in different ways in many papers [7–9]. For example, the achievable color gamut for different types of displays has been studied in detail [8]. Many papers have been published to present methods for color gamut quantification mainly in the printing area [10,11]. The simplest method is to work in the CIE xy 2D space, or better, in the CIE $u'v'$ 2D space. The brightness can also be taken into account in the CIE XYZ 3D space or the $L^*a^*b^*$ 3D space. Using the latter space, color and luminance viewing-angle measurements have been combined to compare the perceptual angles based on the changes in brightness and colorfulness [12,13].

The purpose of this study is to present a full analysis of the color-viewing-angle properties of different displays using different color spaces. First, the classical luminance contrast that does not involve color properties is presented. In the second part, the viewing-angle measurements of the color primaries are used to compute the color gamut of the display in the CIE $u'v'$ 2D space. It is particularly shown that the additional measurement of the binary color states (cyan, yellow, and magenta) improves the accuracy because the black pixels are more correctly taken into account. The third technique is to use the white- and black-state color measurements in addition to the others, to work in the $L^*a^*b^*$ 3D space. The convex hull color volume is computed for each viewing angle, and its main characteristics are derived for the full viewing angle. The advantages of the different techniques are discussed and compared for different kinds of displays.

*Corresponding author. Email: pboher@eldim.fr

ISSN 1598-0316 print/ISSN 2158-1606 online

http://dx.doi.org/10.1080/15980316.2011.621313
http://www.tandfonline.com

2. Experiment

2.1. *Viewing-angle measurement system*

The EZContrastXL88 viewing-angle measurement system is based on Fourier optics to collect all the light coming from the display. The first objective is to provide an image of the angular emission of the display in a Fourier plane. This objective can be quite complicated, especially when its angular aperture is very high. The maximum angle measurable with the EZContrastXL88 system is ±88°. A field lens is then used to bend the rays toward a second objective. An additional role of this lens is to conjugate the plane of the display and the plane of an iris. This iris is used to control the size of the measurement spot (maximum size for the EZContrastXL88 system: 2 mm) independently of the angular aperture. The second objective is used to image the Fourier plane on the surface of the CCD. The system is achromatic in the visible range, and the incidence on the different lenses is minimized to avoid polarization effects. The camera is a high-resolution monochrome 16 bit CCD sensor Peltier cooled at −20 °C. To achieve accurate luminance and color measurements, the system uses optical filters and a specific design and calibration [14]. At first, the spectral response of the system is measured with regard to a reference photodiode calibrated by NIST. Then the design of the dedicated color filters is made to match the CIE curves as closely as possible. Generally, five color filters are used to match the three CIE curves (2 for X, 2 for Y, and 1 for Z). The accuracy of the luminance measurements is lower than ±3% in the entire chromatic plane. The accuracy of the chromaticity is also lower than ±0.005 [6]. Additional color calibration methods are also available to increase the color accuracy depending on the target [6]. This accuracy is slightly smaller than what is obtained using a best-quality spectrophotometer (±2% on luminance and ±0.003 on chromaticity), but for only one angle and for a much larger angular resolution (2° compared with 0.3° for Fourier optics). It is why Fourier-optics instruments are widely used for viewing-angle color evaluation.

2.2. *Displays under testing*

The results of the measurements done on four different displays are reported hereafter. These displays are commercial products that are taken only as examples and do not represent all the available technologies. The following displays were used:

- a 47-in LCD CCFL TV from SHARP (Aquos model);
- a 40-in LCD LED edge TV from Philips (40PFL86005H model);
- a 43-in PDP TV from Samsung (PS43D450 model); and
- an 11-in OLED TV from Sony (XEL-1 model).

These four displays represent three main technologies that are presently available in the market: LCD, PDP, and OLED. For the LCD technology, one standard TV with CCFL backlight and one LED edge TV that has very different color properties due to the variable nature of the backlight emission were selected.

2.3. *Example of color measurement*

All the displays were set to the standard configuration conditions that are preferentially used by the customers. Additional features such as green options that adjust the backlight level to the image content were disabled. The displays were warmed up for almost half an hour prior to the measurements to ensure good stability. In each case, color-viewing-angle measurement was achieved at the display center for the following states:

- white state;
- black state;
- three primary color states (blue, green, and red); and
- three binary color states (cyan, yellow, and magenta).

The corresponding measurements for the LCD CCFL TV are reported in Figure 1. The three binary color states are not mandatory for the color analysis, whose results are reported hereafter. The cyan, yellow, and magenta states can be recomputed assuming that cyan = blue + green, yellow = green + red, and magneta = red + blue, but the corresponding data are not exactly equivalent to the direct measurements as they do not take into account the influence of the black pixels, which can be important (see, for example, the light leakage that occurs on the LCD CCFL TV in Figure 1 along the 45, 135, 225, and 315° azimuths). This observation is not valid for PDP or OLED displays, where the black state is near-perfect.

3. Results and discussion

3.1. *Luminance contrast*

The luminance contrast is easily computed based on the ratio of the white- and black-state luminance measurements. The results obtained from the two LCD displays are reported in Figure 2. Indeed, the luminance contrast does not mean anything for OLED or PDP displays, where the black state is quasi-perfect. The maximum contrast is always on-axis and is quite different depending on the display. More important is the angular aperture, which maintains a high contrast. The iso-level curves for a contrast of 500 are also reported in Figure 2 for easier comparison. It can be clearly seen that the LCD LED edge has the best luminance contrast horizontally. On the contrary, the LCD CCFL display is much more limited in terms of luminance contrast.

3.2. *Analysis in the chromatic plane*

The standard chromatic plane is the CIE *xy* plane derived directly from the *XYZ* CIE measurements. The use of the

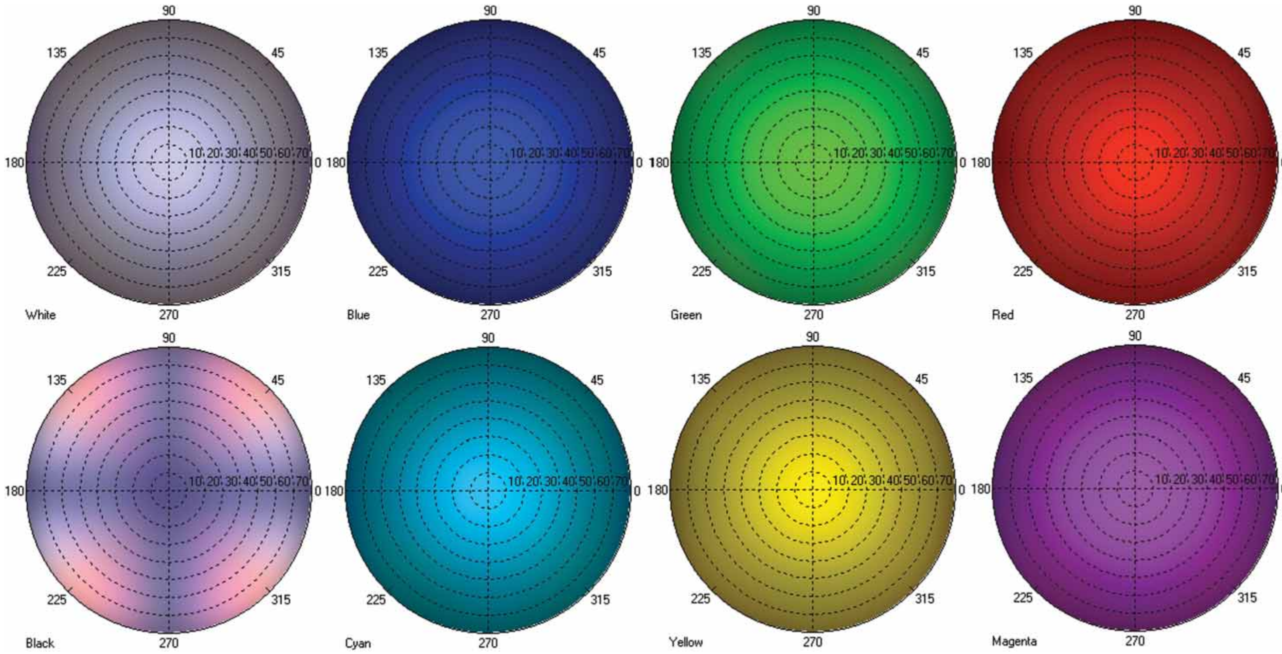

Figure 1. Color measurements on the LCD CCFL TV for the white and black states, the three primary colors blue, green, and red, and the binary colors cyan, yellow, and magenta. The data are represented in false colors in the Fourier plane vs. the incidence and azimuth angles.

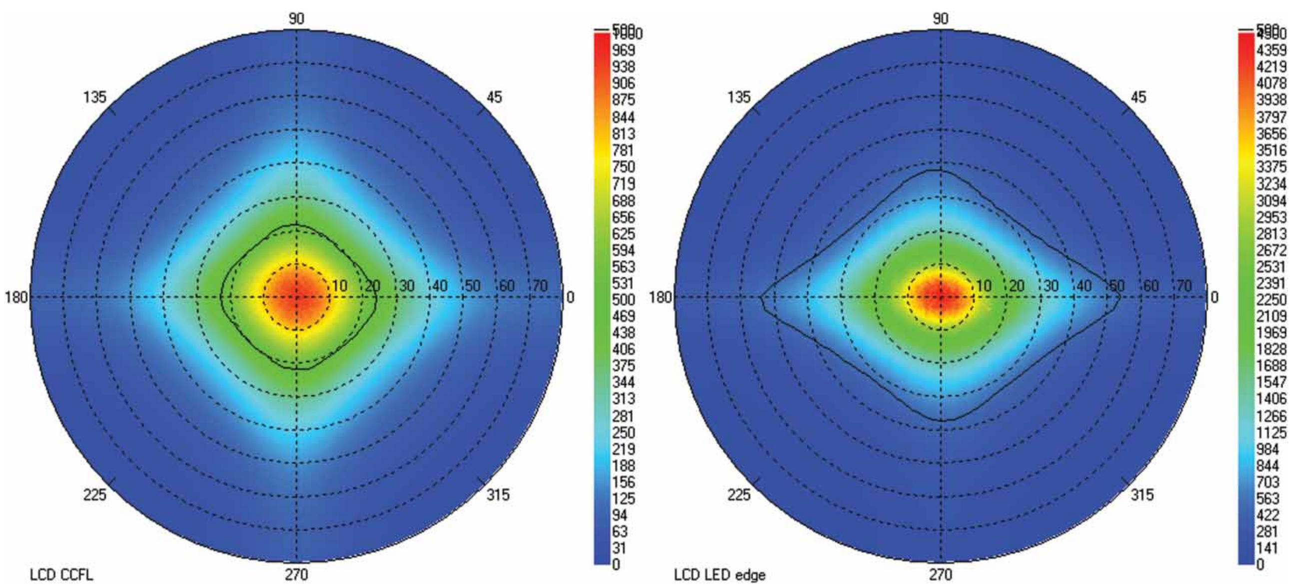

Figure 2. Luminance contrast of the two LCD displays: the iso-level at 500 is reported in the figures.

more uniform CIE $u'v'$ color space is nevertheless preferred

$$u' = \frac{4X}{X + 15Y + 3Z}, \quad v' = \frac{9Y}{X + 15Y + 3Z}.$$

The color gamut can then be computed for each viewing angle by evaluating the area of the polygon defined by the three color primaries and the binary combinations of color primaries (cf. Figure 3). In the case of a display with R, G, and B pixels, the influence of the black pixels can be particularly detected for high incidence angles, where the light leakage of the black pixels is non-negligible compared with the emission of the other pixels. An example is shown in Figure 3. The data taken on-axis or at 70° incidence horizontally from the LCD LED edge display give a quasi-perfect color triangle in the $u'v'$ space. For these viewing angles, the light leakage of the black state is very limited, and so the black pixels do not play a role. On the contrary, much more light leakage is occurring along the 55° azimuth, and so the influence of the black pixels is easily detected on the polygon of Figure 3(b). A correct estimation of the

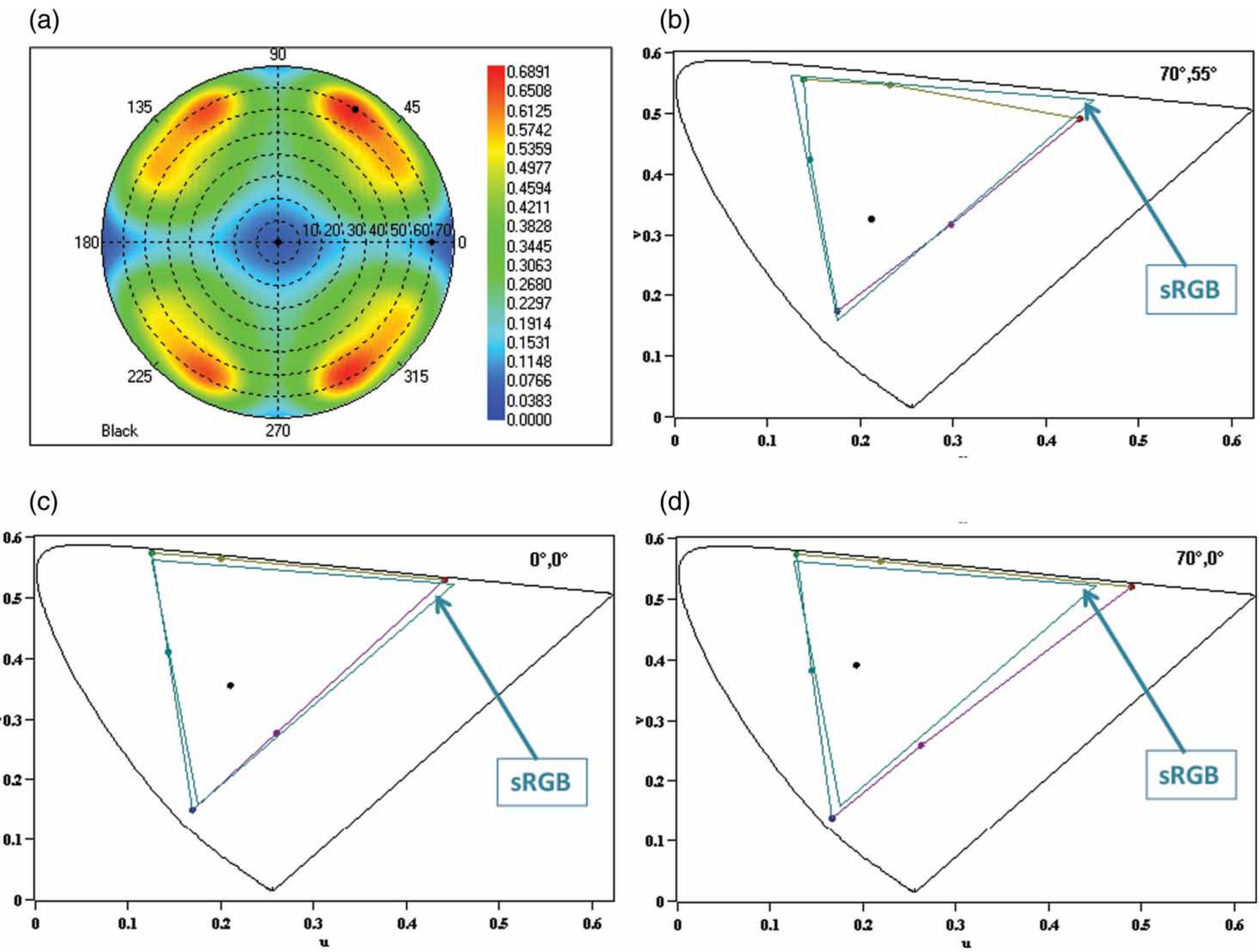

Figure 3. Black-state luminance (a) and color gamut for the LCD LED edge seen on-axis (c) and at 70° incidence horizontally (d) and at 55° azimuth (b), reported in the u'v' chromatic plane. The influence of the light leakage on the color gamut is seen at the 0° or 55° azimuth angles. The sRGB triangle is also shown.

color gamut in these conditions requires the measurement of the binary combinations of color primaries in addition to the color primaries. The color gamuts measured on-axis on the four different displays are shown in Figure 4. The gamut of the LCD CCFL display is smaller than that of the sRGB reference [16]. That of the LCD LED edge display is larger. The two other displays show much higher gamuts, but for different reasons. The PDP display shows very good blue and red components while the OLED display shows an excellent green component.

The color gamut was calculated for all the angles for the four displays. The results, normalized to the sRGB reference, are summarized in Figure 5. The two LCD displays show comparable performances, with a higher gamut horizontally. The two other displays show much higher gamuts, but without clear variations inside the viewing cone. The best display is the OLED TV for its high gamut at all the angles. The gamut stability *vs.* angle is not a guarantee that the color properties do not move in the viewing cone. The white state is more or less sensitive to the angles depending on the display technology. The color difference for the white state is reported in Figure 6 to illustrate this point. Strong variations are observed for the LCD displays and the OLED display. They can be related to the transmittance variation of the liquid crystal cell for LCDs, and to the multilayer structure of the OLED display.

3.3. *Analysis of the L*a*b* volume*

Chromatic-plane coordinates such as the CIE1976 (u'v') or CIE1931 (x,y) coordinates, however, cannot fully represent the chromatic characteristics as they do not include the brightness factor. These planar systems measure the change in the color coordinates but not necessarily how much the perceived color changes, due to the absence of the brightness factor. Even though CIE *XYZ* is very useful as a base definition of absolute color, it has poor performance in predicting the differences between colors. Two color pairs with the same difference in their CIE *XYZ* coordinates can have a very different perceived difference. Several attempts

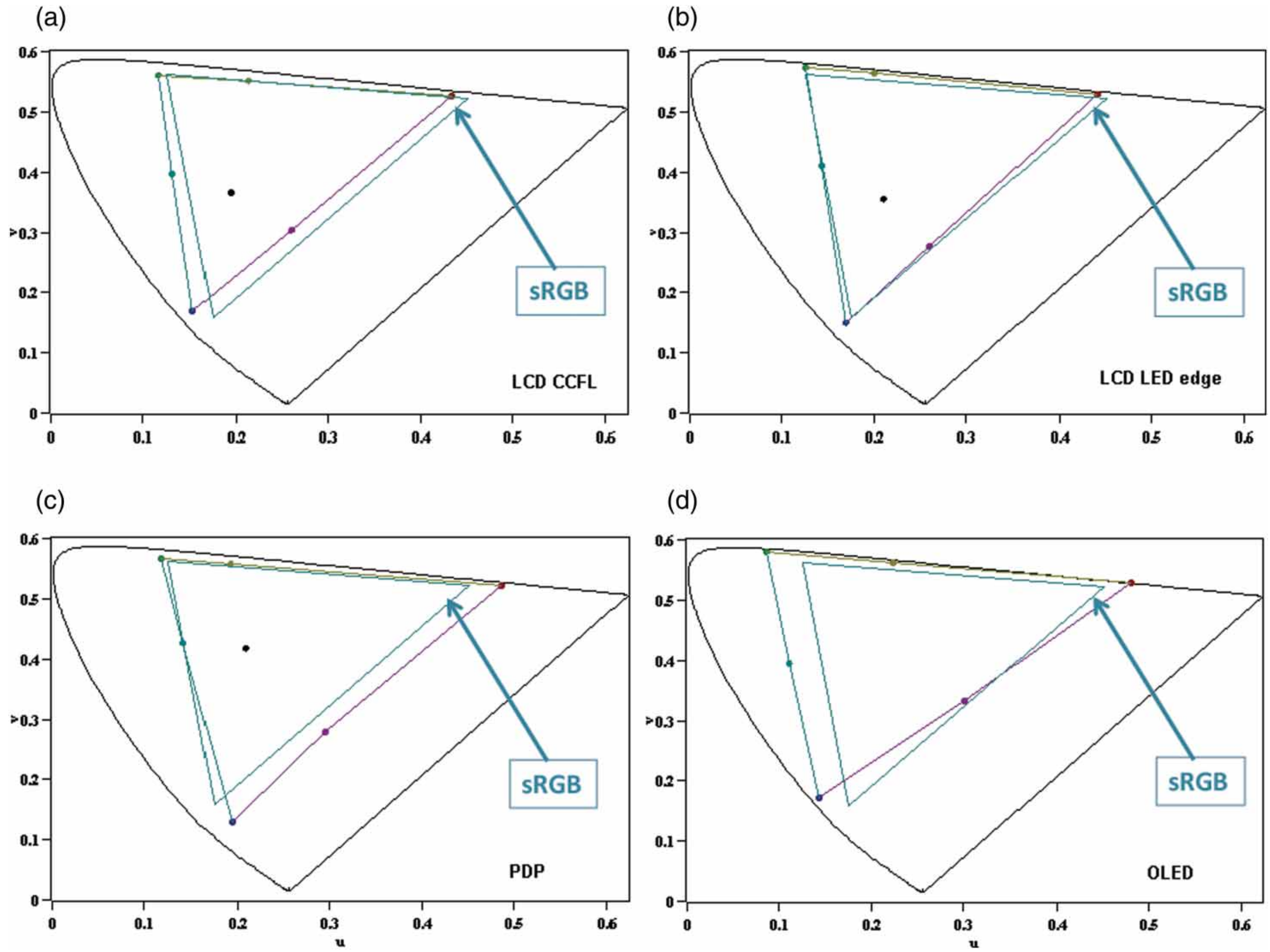

Figure 4. Color gamut reported in the $u'v'$ chromatic plane for on-axis for the four displays. The sRGB triangle is also shown.

to quantify and capture the perception of color differences have been made over the years. The CIE Lab color space is a derivative of the CIE *XYZ* color space [15], in which the coordinates of a color can be calculated using

$$L^* = 116f\left(\frac{Y}{Y_R}\right) - 16,$$

$$a^* = 500\left[f\left(\frac{X}{X_R}\right) - f\left(\frac{Y}{Y_R}\right)\right],$$

$$b^* = 200\left[f\left(\frac{Y}{Y_R}\right) - f\left(\frac{Z}{Z_R}\right)\right],$$

where

$$f(x) = x^{1/2} \quad \text{if } x > \left(\tfrac{6}{29}\right) \quad \text{and}$$

$$f(x) = \tfrac{1}{3}\left(\frac{6}{29}\right)^2 x + \tfrac{4}{29} \quad \text{otherwise}$$

X_R, Y_R, and Z_R are the tristimulus values of the reference white. The L^* dimension represents the perceptual-measure lightness, the a^* dimension represents a perceptual uniform color transition from red to green over gray, and the b^* dimension represents a perceptual uniform color transition from blue to yellow over gray. It is useful to select the on-axis white state as a reference white to check the influence of the viewing angles. To compare different displays, one possibility is to use the on-axis white state of one of the displays as reference. A given illuminant can also be selected. One example of a $L^*a^*b^*$ color volume computed for the LCD CCFL display for the on-axis values using the white state as reference is reported in Figure 7. The sRGB reference volume is also reported for comparison on the cross-section view [16]. The $L^*a^*b^*$ color volumes and some cross-sections of the four displays for the on-axis values are reported in Figures 8 and 9 using the on-axis value as a reference. The shape of the different volume is clearly different even if the volume seems comparable. It is then necessary to compute some parameters associated with each volume for better comparison.

3.4. *Parameters associated with the color volumes*

Each color volume can be characterized by a set of parameters, as reported hereafter. For each $L^*a^*b^*$ volume, different

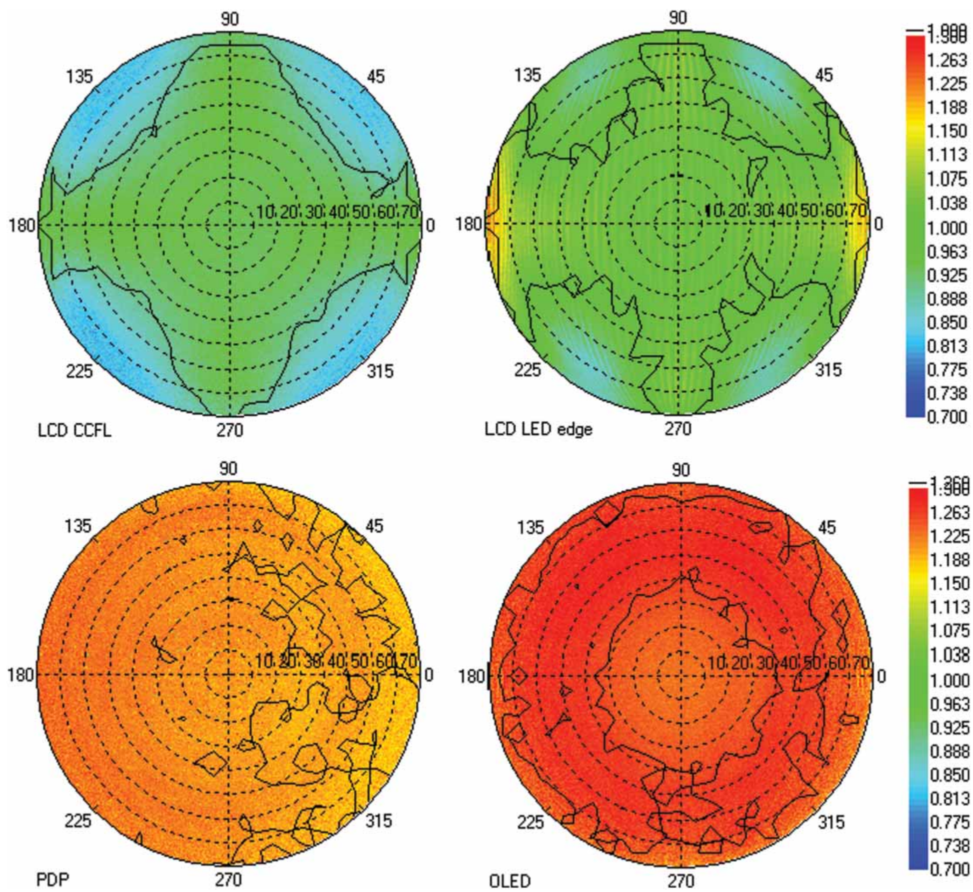

Figure 5. Color gamut ratio *vs.* sRGB gamut *vs.* viewing angle in the *u*'*v*' chromatic plane. The iso-level curves are 0.9 for the LCD CCFL display (top left), 1.0 for the LCD LED edge display (top right), 1.2 for the PDP display (bottom left), and 1.26 for the OLED display (bottom right).

horizontal cross-sections are automatically computed (see some examples in Figure 9). These cross-sections are used to evaluate volume V. Each section is approximated by a series of segments delimited by $N(a_i, b_i)$ points. Surface A of each cross-section is approximated by the sum of N irregular polygons [17], as follows:

$$A = \tfrac{1}{2}\sum_{i=0}^{N-1}(a_i b_{i+1} - a_{i+1} b_i).$$

In addition, the gravity center of each cross-section (a_m, b_m) is computed using the same polygonal decomposition [17] (the trajectories of the gravity center are also shown in Figure 9).

$$a_m = \frac{1}{64}\sum_{i=0}^{N-1}(a_i + a_{i+1})(a_i b_{i+1} - a_{i+1} b_i) \quad \text{and}$$

$$b_m = \frac{1}{64}\sum_{i=0}^{N-1}(b_i + b_{i+1})(a_i b_{i+1} - a_{i+1} b_i).$$

The overall gravity center, and in particular its lightness $L^*{}_G$, chroma $C^*{}_G$, and hue angle $h^*{}_G$, are deduced

$$C^* = \sqrt{a^{-2} + b^{-2}},$$
$$h^* = \arctan[b^*/a^*].$$

The calculation of the surface of the hull S is made using a list of corner points that are the facets of the hull. The area of the hull is the sum of the area of the respective individual triangles. This surface can be normalized to the surface of the sRGB reference volume. A very intuitive measure of the evenness of a body is to relate the surface area of the body to some relevant reference area. This value was compared with that of a sphere of the same volume calculating area quota, AQ, as follows [18]:

$$\mathrm{AQ} = \frac{S}{S_{\mathrm{sphere}}} = \frac{S}{4\pi\left(\sqrt[3]{3V/4\pi}\right)^2}.$$

3.5. *Viewing-angle dependence of the L*a*b* color volume*

The different parameters of each $L^*a^*b^*$ volume were computed at the different viewing angles for the four displays.

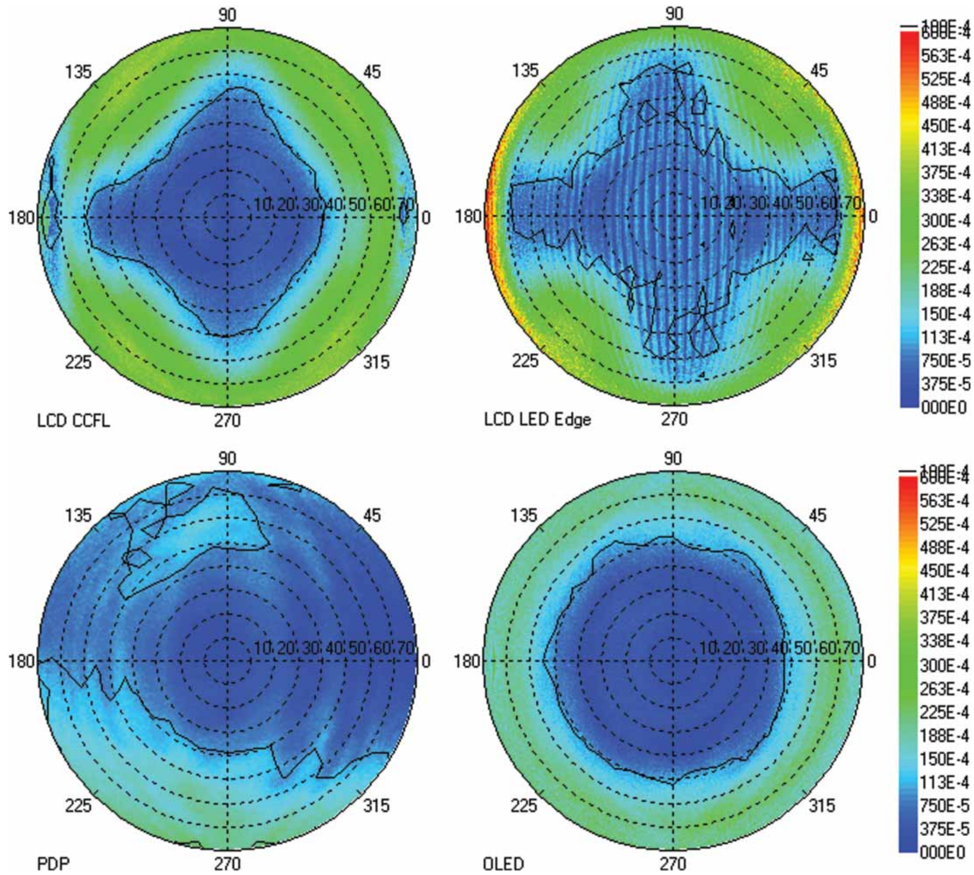

Figure 6. Color difference for the white state with regard to the on-axis value in the u'v' chromatic plane. The iso-level curves are for a difference of 0.001.

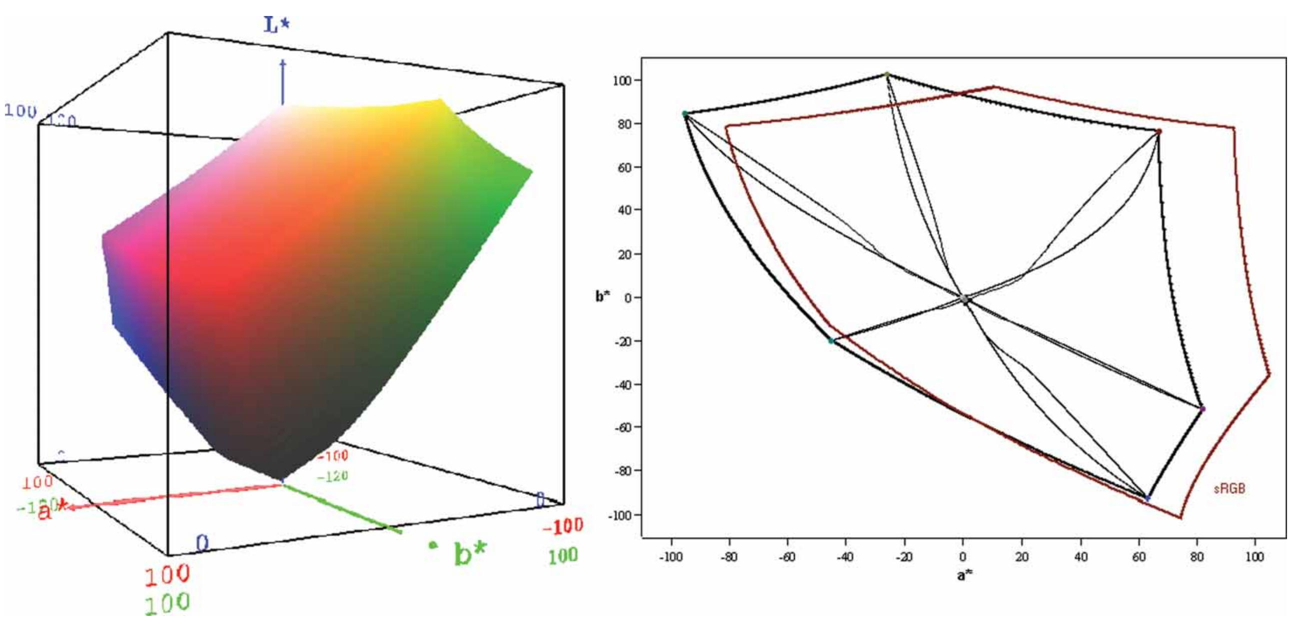

Figure 7. $L^*a^*b^*$ color volume of the LCD CCFL display for on-axis measurements (left) and the corresponding maximum a^*b^* cross-section (right). The projections of the different volume edges in the a^*b^* plane are also shown (right).

Some of them are reported in the following. The color volume relative to the sRGB reference is shown in Figure 10. It follows the same trends as those of the color gamut shown in Figure 5, but with some important differences. The largest color volume is obtained for the OLED display, but the reduction with the incidence angle is more

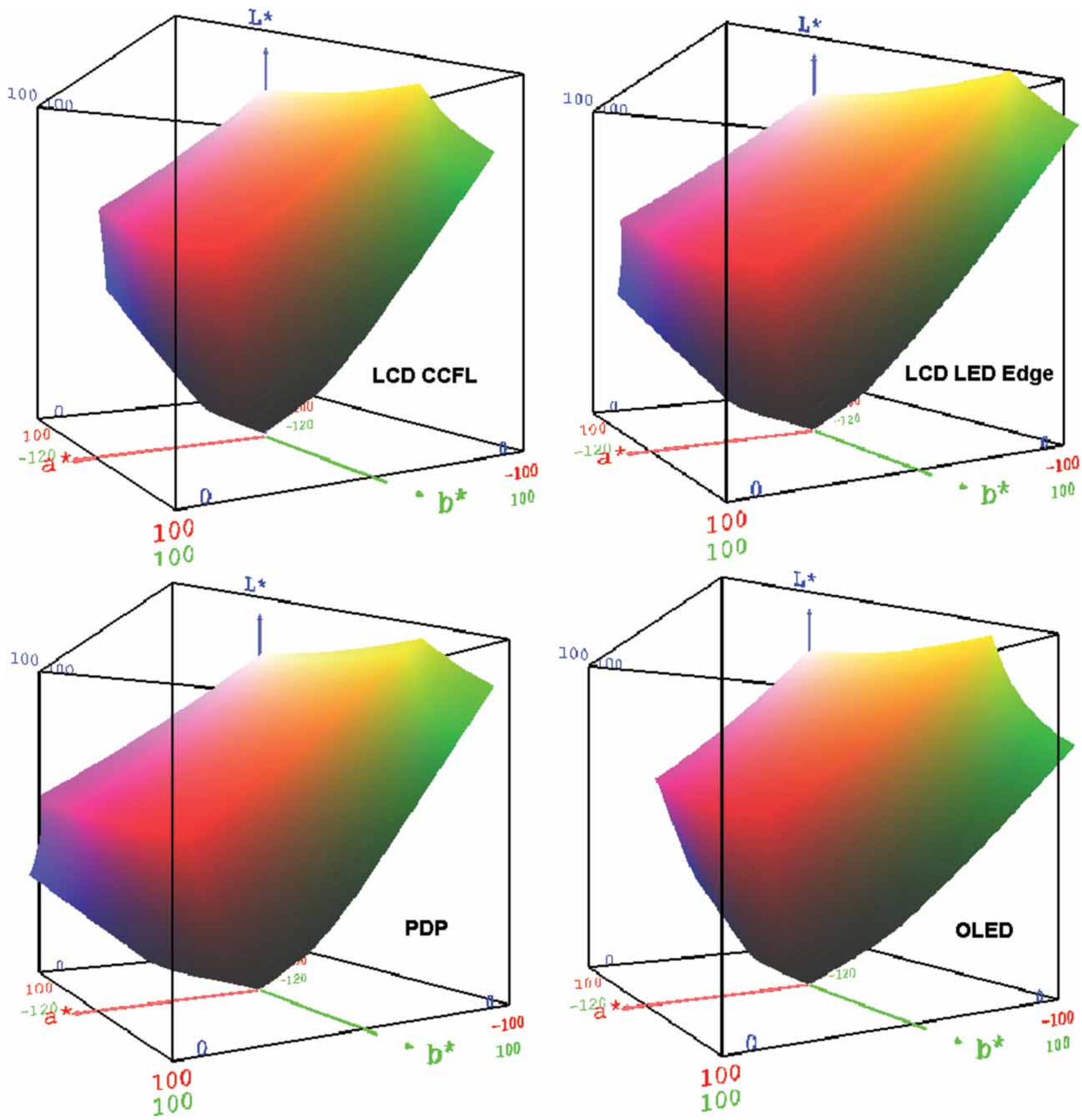

Figure 8. $L^*a^*b^*$ color volume on-axis for the four different displays. The reference is taken as the white-state measured on-axis for each display.

important compared with the PDP display when the gamut is relatively stable (cf. Figure 5). This is due to the reduction in the luminance when going outside the normal range, as also observed in the LCD displays. The surface relative to the sRGB reference follows the same behavior as that of the volume, but the reduction is less important at a high incidence angle for all the displays, except for the PDP display, where it is very stable. This is not surprising as PDP displays do not suffer *a priori* from viewing-angle problems. For the OLED display, even if the color volume is higher at normal incidence, the incidence angle behavior is important but very isotropic. These differences can be easily seen in the area quota behavior of the four displays (cf. Figure 10).

The angular behavior of the gravity center of the color volume is summarized in Figure 11, where the lightness, chroma, and hue behaviors are reported. The region where L^*_G is higher than 50 is comparable for the two LCD displays and the OLED display. It is higher for the PDP display. The chroma is lower than 10 for all the angles of the PDP display. Important variations due to the liquid crystal are observed for the two LCD displays. The chroma is high near the normal incidence for the OLED display. In addition, strong isotropic variations are observed *vs.* the angle. These observations are confirmed by the hue behavior (cf. Figure 11). The mean hue value gives the global color shift of the OLED display toward green for the LCD displays, yellow for the OLED display, and cyan for the PDP display.

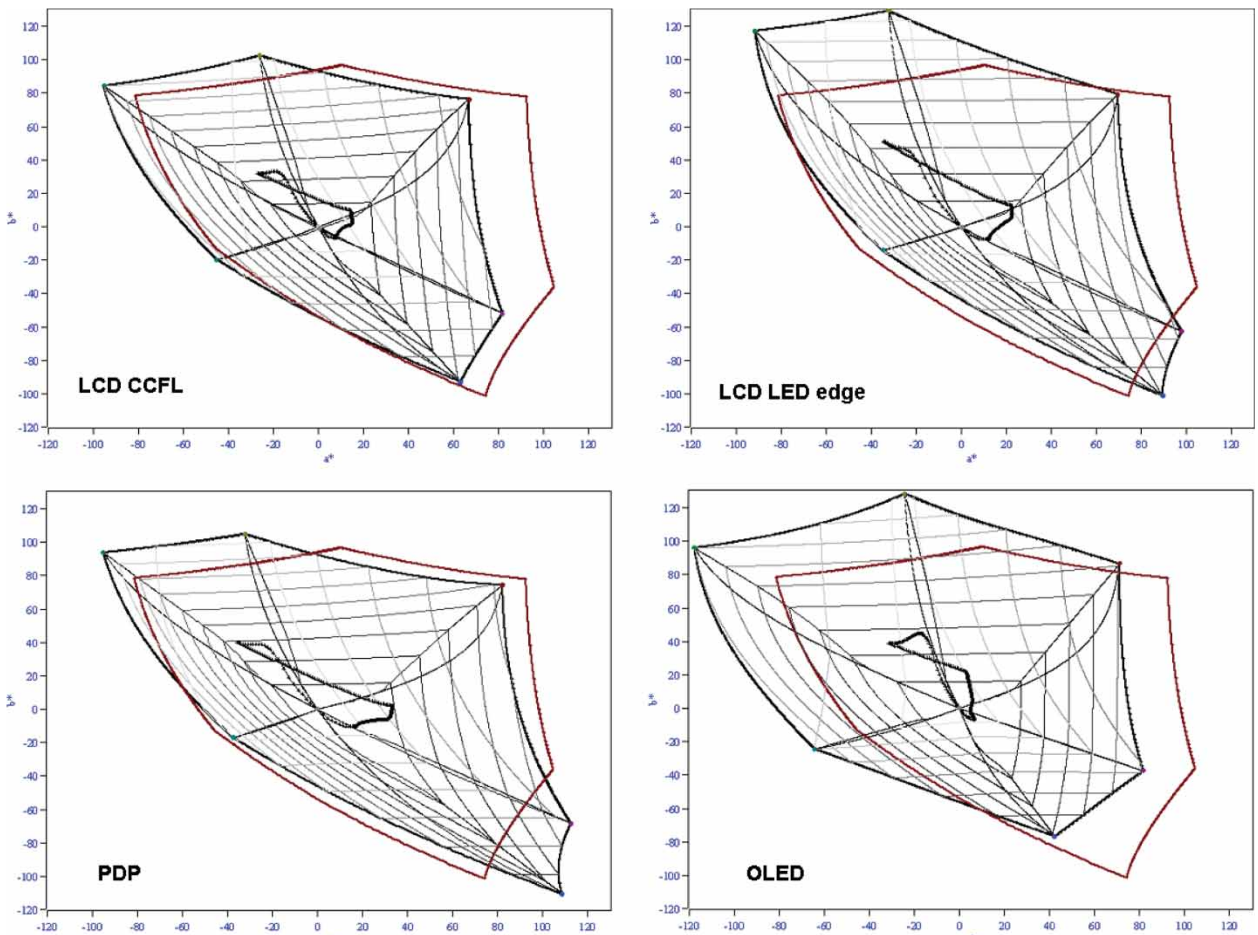

Figure 9. Cross-sections of the $L^*a^*b^*$ color volume measured on-axis for the four displays. The reference is taken as the white state, and the maximum vertical cross-section of the different volume and of the sRGB reference volume, the projections of the different volume edges, and the trajectory of the gravity center of some cross-sections are shown.

4. Conclusions

A full color analysis of different displays using Fourier-optics viewing-angle measurements was presented. A summary of the main characteristics extracted during this study for the four different displays is provided in Table 1. The following comments can be made on the luminance and standard gamut analysis results:

- In terms of the luminance of the white state, the LCD CCFL and OLED displays show the best characteristics on-axis, but the most stable emission in angle is obtained for the PDP display. The poor luminance of PDP is more due to the green concerns and limited consumption than any other reason.
- The luminance contrast is limited for LCD displays compared with the other technologies but is quite high compared with what was achieved three or four years ago. The improvement of the LCD structure has now reached a level that is sufficient for TV applications. The best displays in terms of luminance contrast are the PDP and OLED displays, but this does not mean anything as the black state of these displays are near perfect. Thus, the luminance contrast can no longer be a quality criterion.
- The color stability of the white state is excellent for the OLED display and is also comparable for the other displays.
- The main difference between the displays is probably the color gamut, which is limited for LCD CCFL, medium for the LCD LED edge, and excellent for PDP and OLED. Nevertheless, the four displays do not present a strong variation of the gamut *vs.* angles, and such angular analysis of the color properties is quite limited.

The combined analysis of the luminance and color properties using the $L^*a^*b^*$ color space allows a more precise comparison of the displays. The $L^*a^*b^*$ color volume was computed for each angle. To check the angular dependence of the light emission and to compare the different displays, the use of different characteristics of this color volume is suggested. The following comments can be made on these

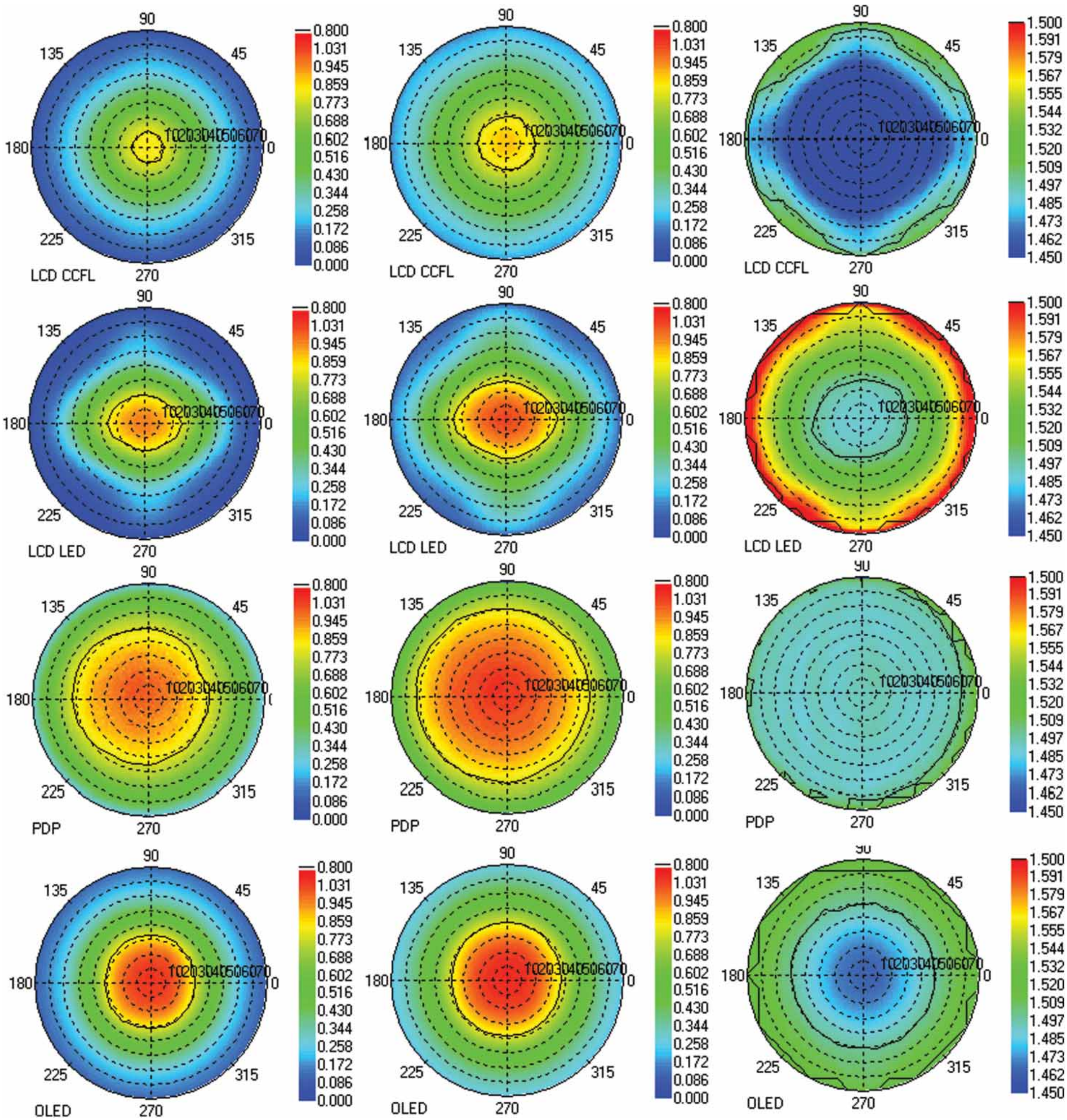

Figure 10. $L^*a^*b^*$ volume ratio to sRGB (left), surface ratio to sRGB (center), and area quota (right) for the four displays. The values are referenced to the white-state on-axis values of each display. The iso-curves are for a ratio of 0.8 for the sRGB ratios and 1.5 for the area quota.

new parameters (cf. Table 1):

- The $L^*a^*b^*$ color volume gives a better idea of the capacity of the display to reproduce colors in the gamut as the luminance is taken into account. The hierarchy of the four displays is nevertheless the same. The LCD CCFL display exhibits a poor color volume that decreases rapidly with the angle. The OLED display appears slightly better than the PDP display, but with much less angular stability. Using only color gamut, the four displays were quite comparable.
- The area of the hull and the area quota support the same conclusions as those relating to the $L^*a^*b^*$ color volume. The occurrence of a large volume for the color volume even for high incidence angles is

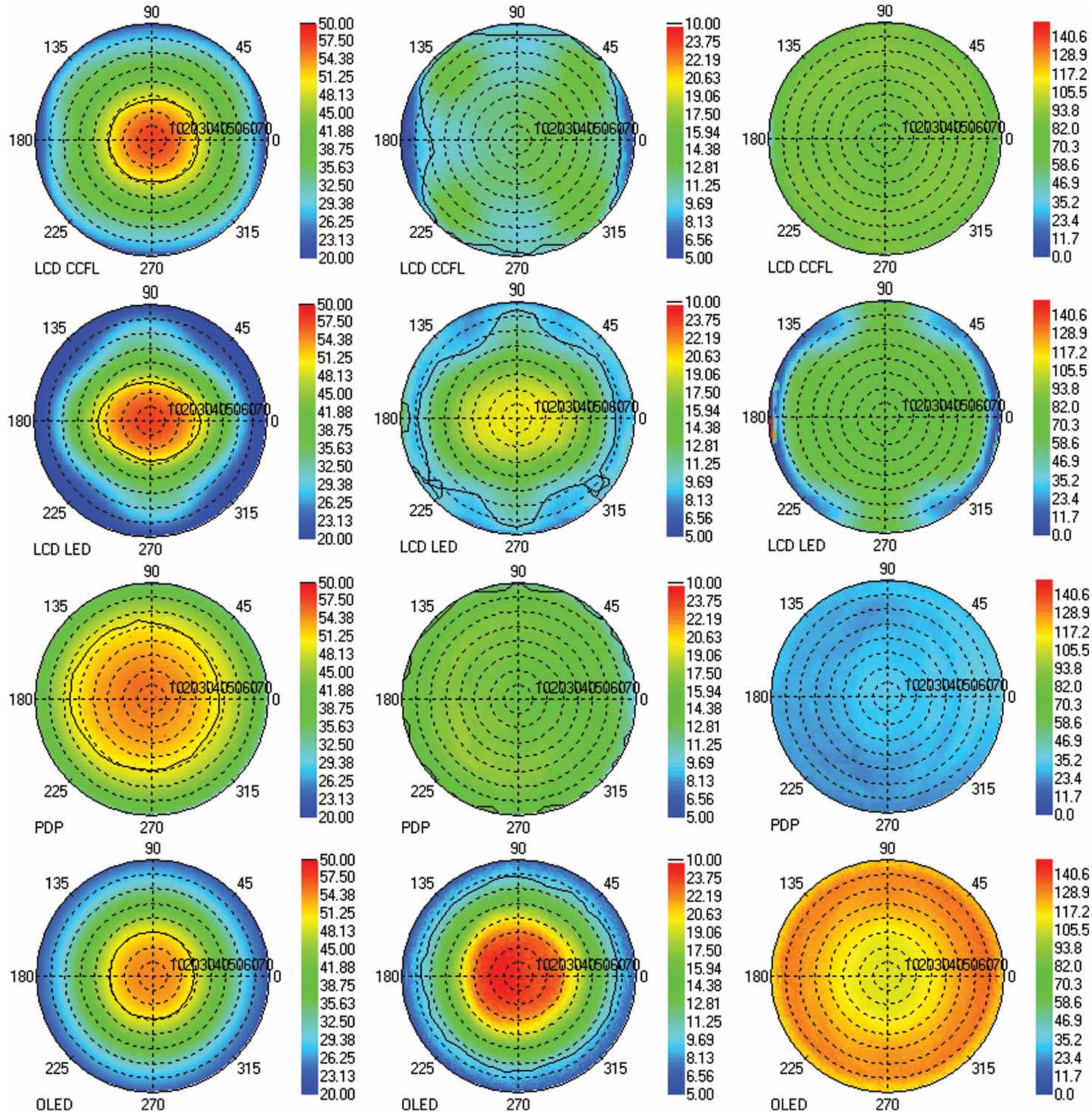

Figure 11. $L^*a^*b^*$ volume gravity center lightness (left) , chroma (center), and hue (right) for the four displays. The values are referenced to the white-state on-axis values of each display. Iso-levels at 50 and 10 are reported for lightness and chroma, respectively.

important, but the color hull must also be stable, without too important color deviations. In addition, the area quota, which indicates how much larger the hull of the color gamut is in relation to an equal volume sphere, is certainly very dependent on the type of emissive spectrum used by the display.

- The gravity center of the color volume is representative of an overall color shift of the display emission with regard to the on-axis emission and, in particular, the chroma and hue of the gravity center. In this respect, LCD CCFL is better optimized than the LCD LED edge, as seen in the amplitude of the chroma and the stability of the hue. On the other hand, the OLED display exhibits unbalanced light emission due to the poor quality of the blue emission compared with the red and green emissions. This imperfection is probably due to the degradation *vs.* lifetime of the blue emission as the display under testing had been used for a long time before the measurements herein were made.

Table 1. Summary of the main characteristics of the four different displays.

Parameter	Display	LCD CCFL	LCD LED Edge	PDP	OLED
Luminance on-state (cd/m^2)	On-axis	386	255	114	356
	Max angle for 50%	40°	45°	67°	44°
Luminance contrast	On-axis	997	4500	6800	$> 200,000$
	Max angle for 500	23°	25°	All	All
Color on-state	x on-axis	0.278	0.272	0.288	0.289
	y on-axis	0.271	0.275	0.300	0.276
	Chromaticity S.dev. for 0-60°	2.188	2.269	2.625	1.674
$u'v$ color gamut	On-axis	0.948	1.026	1.22	1.22
	S.dev. for 0–60°	0.009	0.02	0.02	0.02
$L^*a^*b^*$ volume	On-axis	0.85	0.958	0.978	1.05
	Max angle for 0.8	10°	26°	52°	32°
Area of hull	On-axis	0.892	1.02	1.04	1.06
	Max angle for 0.5	47°	54°	77°	51°
Area quota	On-axis	1.411	1.333	1.494	1.465
	S.dev. for 0-60°	0.017	0.071	0.001	0.015
L^* gravity center	On-axis	57.8	58.11	55.6	54.8
	Max angle for 50	32°	22°	46°	30°
Chroma gravity center	On-axis	12.49	19.58	15.5	24.2
	S.dev. for 0–60°	1.02	2.25	0.98	4.06
Hue gravity center	On-axis	81°	50.1°	32.8°	108.6
	S.dev. for 0–60°	2.6°	13.2°	2.82°	7.4°

Note: The incidence angles are taken horizontally, and the gamuts, volumes, and areas are normalized to sRGB values. The $L^*a^*b^*$ space is always for a reference taken as the on-axis value. S.dev. means standard deviation.

The use of Fourier-optics viewing-angle measurements allows the computation of all the aforementioned characteristics for many incidence and azimuth angles, and a most precise comparison of the displays.

References

[1] T. Leroux, Proc. EURODISPLAY, 1993, pp. 447–449.

[2] T. Leroux and C. Rossignol, in *SID Proceedings* (Orlando, Florida), 1995, pp. 739–742.

[3] P. Boher, T. Leroux, T. Bignon, and V. Collomb-Patton, in Electronic Imaging (San Jose), Proc. SPIE **7237**, 37 (2009).

[4] P. Boher, T. Leroux, and G.D. Bignon, in *SID*, (Los Angeles, 2008), pp. 1517–1520.

[5] P. Boher, T. Leroux, T. Bignon, and V. Collomb-Patton, in *Electronic Imaging* (San Jose), Proc. SPIE **7524**, 26 (2010).

[6] P. Boher, T. Leroux, and V. Collomb-Patton, in *IDW*, (Fukuoka, 2010).

[7] T. Fiske and L. Silverstein, in *CID International Symposium* (Digest, May, 1999), p. 565.

[8] G. Sharma, Proc. IEEE **90**, No. 7, 605 (2002).

[9] G. Sharma, SPIE **4663**, 20 (2002).

[10] R. Balasubramanian and E. Dalal, Proc. SPIE 3018, 110 (1997).

[11] I. Farup, J. Hardeberg, A. Bakke, S. Kopperud, and A. Rindal, in *Proceedings of IS&T and SID's 10th Color Imaging Conference*, Scottsdale, Arizona, 2002.

[12] E. Lee, J. Chong, S. Yang, H. Lee, M. Shin, S. Kim, D. Choi, S. Lee, H. Lee, and B. Berkeley, IMID Seoul Korea, Paper **46-2**, 979 (2009).

[13] E. Lee, J. Chong, S. Yang, H. Lee, M. Shin, S. Kim, D. Choi, S. Lee, H. Lee, and B. Berkeley, KIDS **11**, No. 1, 17 (2010).

[14] T. Leroux, T. Bignon, E. Chauvat, and P. Boher, in *SID Proceedings*, San Francisco, 2006.

[15] R. Hunter, JOSA **38**, 7, 661, (1948).

[16] IEC 61966-2-1:1999. <http://www.color.org/chardata/rgb/srgb.xalter>.

[17] P. Bourke, University of Western Australia, 1988. <http://paulbourke.net/geometry/polyarea/>.

[18] J. Jenevall, Master thesis, Stockholm, 2003.